

# Prediction of Lymph Node Metastasis with Use of Artificial Neural Networks Based on Gene Expression Profiles in Esophageal Squamous Cell Carcinoma

Takatsugu Kan, MD, PhD, Yutaka Shimada, MD, PhD, FACS, Fumiaki Sato, MD, PhD, Tetsuo Ito, MD, Kan Kondo, MD, PhD, Go Watanabe, MD, PhD, Masato Maeda, MD, PhD, Seiji Yamasaki, MD, PhD, Stephen J. Meltzer, MD, and Masayuki Imamura, MD, PhD, FACS

---

**Background:** The aim of the study was (1) to detect candidate genes involved in lymph node metastasis in esophageal cancers and (2) to investigate whether we can estimate and predict occurrence of lymph node metastasis by analyzing artificial neural networks (ANNs) using these gene subsets.

**Methods:** Twenty-eight primary esophageal squamous cell carcinomas were used. Gene expression profiles of all primary tumors were obtained by cDNA microarray. Lymph node metastasis-related genes were extracted with use of Significance Analysis of Microarrays (SAM). Predictive accuracy for lymph node metastasis was calculated by evaluation of 28 cases by ANNs with leave-one-out cross-n. The results were compared with those of other analyses such as clustering or predictive scoring (LMS).

**Results:** Our ANN model could predict lymph node metastasis most accurately with 60 clones. The highest predictive accuracy for lymph node metastasis by ANN was 10 of 13 (77%) in newly added cases that were not used for gene selection by SAM and 24 of 28 (86%) in all cases (sensitivity: 15/17, 88%; specificity: 9/11, 82%). Predictive accuracy of LMS was 9 of 13 (69%) in newly added cases and 24 of 28 (86%) in all cases (sensitivity: 17/17, 100%; specificity: 7/11, 67%). It was difficult to extract useful information for the prediction of lymph node metastasis by clustering analysis.

**Conclusions:** ANN had superior potential in comparison with other methods of analysis for the prediction of lymph node metastasis. This systematic analysis combining SAM with ANN was very useful for the prediction of lymph node metastasis in esophageal cancers and could be applied clinically in the near future.

**Key Words:** Artificial neural networks—Esophageal cancer—Esophageal squamous cell carcinoma—Lymph node metastasis—Microarray—Supervised learning.

---

The prognosis for esophageal cancer is one of the worst worldwide, in spite of recent advancements in diagnosis and therapy. For the treatment of esophageal cancer patients, surgical treatment,<sup>1</sup> endoscopic resec-

tion,<sup>2</sup> radiation therapy, and chemotherapy<sup>3,4</sup> have been employed independently or in combinations. Lymph node metastasis is a strong independent prognostic factor in esophageal cancers,<sup>5</sup> and therapeutic selections are also influenced by whether lymph node metastasis has already occurred or not. The evaluation of lymph node metastasis before treatment is usually performed with computed tomography (CT) and endoscopic ultrasonography (EUS); however, their sensitivity is not satisfactory.<sup>6</sup> Although it has been reported that detection of lymph node metastasis by positron emission tomography (PET) is superior to that by CT and EUS, it is still insufficient.<sup>7</sup> We need

---

Received March 8, 2004; accepted August 2, 2004.

From the Department of Surgery and Surgical Basic Science, Graduate School of Medicine, Kyoto University, Kyoto, Japan.

Address correspondence and reprint requests to: Yutaka Shimada, Department of Surgery and Surgical Basic Science, Graduate School of Medicine, Kyoto University, Kawaracho 54, Shogoin, Sakyo-ku, Kyoto 606–8397, Japan; Fax: 81-75-751-4390; e-mail: shimada@kuhp.kyoto-u.ac.jp.

Published by Lippincott Williams & Wilkins © 2004 The Society of Surgical Oncology, Inc.

new strategies superior to existing modalities for the detection of lymph node metastasis.

The frequency of lymph node metastasis is different even among individuals with similar extents of primary tumor invasion. This implies that lymph node metastasis of esophageal cancers may be a reflection of different characteristics depending on the diverse gene expression of the tumors, and we may be able to identify candidate genes for lymph node metastasis and to categorize patients according to their lymph-node metastasis status. Here, we report the successful identification of candidate genes related to lymph node metastasis with use of cDNA microarrays and the possibility of prediction of lymph node metastasis in esophageal cancers. If lymph node metastases in esophageal cancers could be predicted, we would have a powerful diagnostic tool that could be applied for designing tailor-made treatments.

With use of microarray technologies, gene expression profiles have been obtained for various malignant tumors,<sup>8</sup> including esophageal cancers.<sup>9</sup> However, it has also been proven difficult to extract useful information accurately and efficiently from this enormous genetic dataset and to use the data effectively in clinical situations. We have to establish useful strategies for treating esophageal cancer patients based on truly useful genetic information from microarray data.

Artificial neural networks (ANNs),<sup>10</sup> which are one of the supervised classification techniques that have supervised learning mechanisms by training data, have a powerful pattern-recognition ability and have been applied to analyze gene microarray data relatively recently.<sup>11</sup> We believe that ANN can successfully recognize complicated relationships among the expression of various genes because gene expression profiles can be indicated as patterns. Candidate genes for lymph node metastasis are first extracted by means of a specified algorithm: significance analysis of microarrays (SAM) (<http://www-stat.stanford.edu/~tibs/SAM/>)<sup>12</sup> that can statistically extract differences of gene expression between two groups. Then, prediction of lymph node metastasis is performed by ANN on the basis of those gene expressions.

We also compared ANN with clustering analysis,<sup>13</sup> which is one of the unsupervised classification methods that do not have learning mechanisms, and with one of the methods for predictive scoring analysis<sup>14,15</sup> reported relatively recently.

## MATERIALS AND METHODS

### RNA Extraction and Patient Profiles

Twenty-eight independent primary tumors from esophageal cancer patients who underwent surgical treat-

ments at Kyoto University Hospital were enrolled in the study during a 12-year period (1990–2001). Written informed consent was obtained from each patient for the operation and for use of their resected samples. All tissue specimens of esophageal squamous cell carcinomas and normal esophageal epithelium at the furthest points from the tumor within the surgically resected specimens were frozen in liquid nitrogen immediately after their removal. Frozen tissues of esophageal cancers from the 28 enrolled patients were crushed into pieces and lysed immediately in TRISOL reagent (Invitrogen Corp., Carlsbad, CA), and total RNA was extracted according to the manufacturer's instructions. mRNA was purified with an Oligotex dT-30 super poly(A) purification kit (TaKaRa Bio, Japan) according to the manufacturer's instructions. For reference probes, mRNA of normal esophageal epithelium from more than 10 patients was mixed and pooled. Clinicopathological information of all patients is shown in Table 1. We included previously reported data in which dissected lymph nodes were stained with AE1/AE3 (anticytokeratin antibody) to precisely detect micrometastasis in lymph nodes.<sup>16</sup>

### Microarray Procedure and Data Processing

Gene expression profiles of all 28 primary tumors were obtained by cDNA microarray. Detailed procedures were as previously described,<sup>9</sup> with the following modifications. In brief, 1.2  $\mu$ g of each extracted mRNA from cancer tissues and pooled reference mRNA were used for fluorescent labeling with Cy5-dUTP or Cy3-dUTP, respectively. Each of the labeled first-strand cDNAs was mixed and hybridized to cDNA microarray chips containing 8064 genes, supplied by the University of Maryland School of Medicine.<sup>17</sup> Commercially obtained slide cover slips (TaKaRa Spaced Cover Glass L) and TaKaRa hybridization chambers specially designed for microarray experiments were used. Fluorescent images were scanned with an Array Scanner 428 (Affymetrix, Santa Clara, CA), and the signal intensities were calculated with ImaGene 4.0 (BioDiscovery, Marina Del Rey, CA). Obtained data were normalized with intensity-dependent normalization.<sup>18</sup>

### Gene Filtering

The gene filtering process was performed with SAM. We estimated the median false discovery rate (FDR), which is the percentage of genes falsely detected as showing statistically significant differential gene expressions by SAM. SAM calculates "d value" as an index of significance with use of an algorithm based on Student's *t*-test and performs data permutations to determine FDR. We applied SAM to two groups: (A) gene expression

TABLE 1. Clinicopathological characteristics

Case	G	A	L	Type	T	N	M	TNM Stage	Lymph Node Dissection	Lymph Node Metastasis	MM
LN(+) <sup>1</sup> **	M	52	Ut	Mod	2	1	1b	4b	29	4 (13.8%)	NP
LN(+) <sup>2</sup> **	M	59	Mt	Mod	3	1	0	3	98	4 (4.1%)	(+)
LN(+) <sup>3</sup>	M	44	Mt	Mod	4	1	1b	4b	29	11 (37.9%)	(+)
LN(+) <sup>4</sup>	M	55	Lt	Well	4	1	0	3	60	8 (13.3%)	(+)
LN(+) <sup>5</sup> **	M	60	Lt	Mod	2	1	0	2b	22	9 (40.9%)	(-)
LN(+) <sup>6</sup>	M	54	Mt	Poor	4	1	0	3	36	6 (16.7%)	(+)
LN(+) <sup>7</sup> **	M	68	Mt	Poor	3	1	1b	4b	36	7 (19.4%)	(+)
LN(+) <sup>8</sup>	M	70	Mt	Well	4	1	1b	4b	17	12 (70.6%)	(+)
LN(+) <sup>9</sup> **	M	81	Lt	Mod	3	1	0	3	53	22 (41.5%)	NP
LN(+) <sup>10</sup> **	M	69	Ut	Poor	2	1	1b	4b	75	17 (22.7%)	NP
LN(+) <sup>11</sup>	M	49	Mt	Poor	4	1	0	3	42	16 (38.1%)	(+)
LN(+) <sup>12</sup> **	M	67	Mt	Well	2	1	1a	4a	48	8 (16.7%)	NP
LN(+) <sup>13</sup> **	M	76	Lt	Poor	3	1	1a	4a	40	22 (41.5%)	NP
LN(+) <sup>14</sup>	F	47	Mt	Mod	1	1	1a	4a	57	11 (19.3%)	NP
LN(+) <sup>15</sup> **	M	58	Lt	Mod	2	1	0	2b	75	14 (18.7%)	NP
LN(+) <sup>16</sup>	M	43	Mt	Mod	1	1*	1b	4b	43	0	(+)
LN(+) <sup>17</sup>	M	68	Lt	Mod	4	1*	0	3	47	0	(+)
LN(-) <sup>1</sup> **	M	54	Lt	Mod	2	0	0	2a	71	0	NP
LN(-) <sup>2</sup> **	M	76	Lt	Mod	3	0	0	2a	45	0	NP
LN(-) <sup>3</sup>	F	78	Ut	Poor	1	0	0	1	58	0	NP
LN(-) <sup>4</sup> **	M	51	Lt	Mod	2	0	0	2a	37	0	NP
LN(-) <sup>5</sup>	F	70	Mt	Poor	1	0	0	1	56	0	(-)
LN(-) <sup>6</sup>	F	72	Lt	Poor	1	0	0	1	39	0	(-)
LN(-) <sup>7</sup> **	M	74	Ut	Mod	3	0	0	2a	50	0	(-)
LN(-) <sup>8</sup>	M	66	Mt	Poor	1	0	0	1	33	0	NP
LN(-) <sup>9</sup>	F	77	Ce	Well	4	0	0	3	94	0	(-)
LN(-) <sup>10</sup> **	M	61	Lt	Poor	2	0	0	2a	53	0	NP
LN(-) <sup>11</sup> **	M	52	Lt	Mod	2	0	0	2a	32	0	NP

T, N, M, and TNM stages are defined according to the fifth edition of the TNM classification of UICC in 1997. G, gender; A, age; L, location; mm, micrometastasis; Ut, upper thoracic; Mt, middle thoracic; Lt, lower thoracic; Ce, cervical; Mod, moderately differentiated; Well, well differentiated; Poor, poorly differentiated; NP, not performed. Lymph node dissection and lymph node metastasis are the numbers at the time of surgery (\* indicates micrometastasis in lymph node; \*\* is used for SAM).

profiles of nine cases with lymph node metastases and (B) gene expression profiles of six cases without lymph node metastasis. All patients in groups A and B were made uniform in T category (T2 or T3 in the fifth edition of the TNM classification of UICC in 1997) to minimize the bias of gene expression influenced by high or low T grade.

### ANN Construction and Testing

Our ANN, which consists of four layers, including two hidden layers, and has a Feed Forward with Error Back-propagation function, was constructed with NEURO-SIM/L software (Fujitsu Limited, Japan) with the gene subsets extracted by means of SAM. The schema of our ANN is shown in Figure 1. The number of neurons in the input layer was equal to the number of genes used, and the ideal outputs were set at +1 for the presence of lymph node metastasis and at 0 for absence of lymph node metastasis. Predictive accuracy, which was defined as the number of true positives plus true negatives divided by total number of cases, was calculated by the evaluation of newly added cases and of all 28 cases in

ANN with leave-one-out cross-n using various numbers of genes. Leave-one-out cross-n is defined as a “k-fold cross-n” technique in which the data are divided into k subsets of equal size and the whole data sets are cross-d. If k equals the sample size, this is called “leave-one-out cross-n.” The areas under the receiver operating characteristic curve (Az) were also calculated with use of publicly available software (WROCFIT ROC curve fitting ver.1.44; Wataru Ogawa, Japan) to evaluate the prediction models for lymph node metastasis.

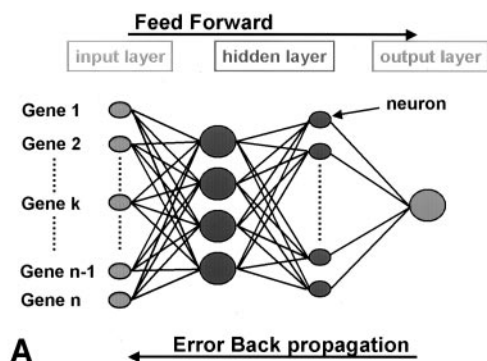
The schematic diagram of this study is shown in Figure 2.

### Predictive Formula for Discrimination of Lymph Node Metastasis

From the results obtained using SAM, we set the d value as the discriminant coefficient (*dj*) of a predictor gene (*j*). A lymph node metastasis score (LMS) of each sample (*i*) was calculated with the following formula:

$$LMS_i = \sum dj \times \log_2 rij$$

Artificial neural networks (ANNs) (1)



Artificial neural networks (ANNs) (2)

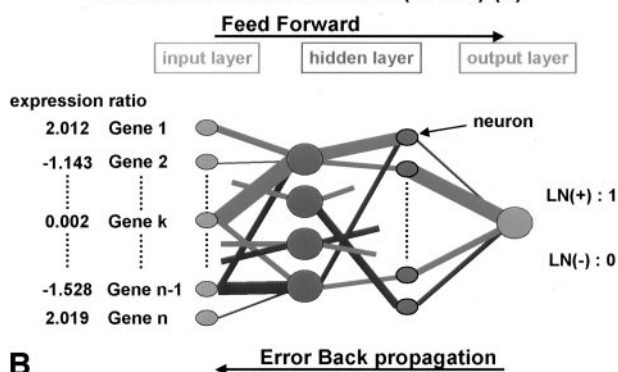


**FIG. 1.** A schematic representation of our artificial neural networks (ANNs). ANNs typically have an input layer, one or more hidden layers, and an output layer. Our ANN has two hidden layers; the first hidden layer has four neurons and the second hidden layer has 10 neurons (bottle-neck type). A: Each neuron is connected with weights randomly in an initial state. B: During the learning process, the ANN is presented with a training set (cDNA microarray data in this study) and is taught the correct diagnosis or output, which is encoded by numbers (lymph node metastasis-positive state is encoded by 1 and -negative state by 0). Data from each ANN layer pass to the next one until they reach the output. The ANN diagnosis is compared with the ideal diagnosis, and an error is generated. The error is backpropagated through the ANN, and the weights of the connections between the neurons are adjusted in an attempt to decrease this error. Once this backpropagation reaches the input layer, another wave of forward-processing begins and reaches the output layer again. This iterative learning process occurs until the ANN is able to make an accurate diagnosis of the training set. After training, the ANN is presented with new microarray data in a test set that has not been used by the ANN.

where  $r_{ij}$  is the expression ratio (Cy5/Cy3) of gene ( $j$ ).

**Hierarchical Clustering**

Gene expression data were manipulated and clustered with use of established algorithms implemented in the publicly available software program Cluster.<sup>13</sup> Average linkage clustering with centered correlation was used. The clustering result was visualized with TreeView software.<sup>13</sup>

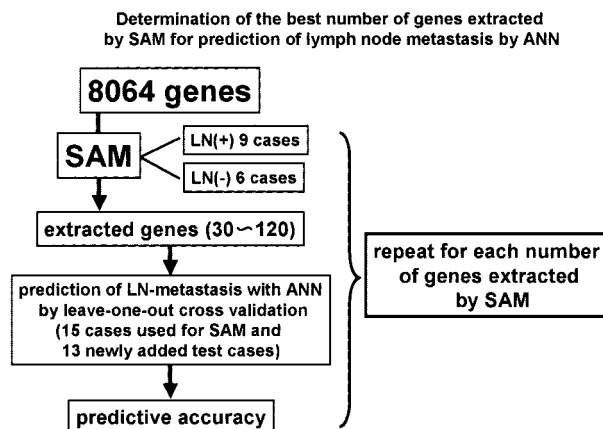


**FIG. 2.** A schematic flow chart for determining the best gene subset for prediction of lymph node metastasis with use of the ANN in our study. Nine cases with lymph node metastasis and six cases without lymph node metastasis were selected for SAM, and candidate genes were extracted from 8064 genes. Thirteen cases were newly added, and a total of 28 cases were evaluated for lymph node metastasis with use of ANN by leave-one-out cross-n. Each gene subset extracted with SAM was tested with ANN, and the best gene subset for prediction of lymph node metastasis was determined (LN = metastasis; LN(+) = lymph node metastasis-positive; LN(-) = lymph node metastasis-negative).

**Validation For Microarray Data**

Semiquantitative reverse transcriptase polymerase chain reaction (RT-PCR) was performed with LightCycler (Roche Molecular Biochemicals, Mannheim, Germany)<sup>19</sup> as the validation for microarray data. Desmuslin (DMN) and interferon gamma receptor 1 (IFNGR1) were used, because these genes were expressed differentially among samples. The primer sequence sets were designed with primer analysis software (OLIGO 4.0-s),<sup>20</sup> and optimal annealing temperatures were as follows: DMN, 5'-CATT-TGTGCTTGCTGGTTCA-3', 5'-TTAAGGCCCTTTGGA-TGTTGG-3', 56.4°C; IFNGR-1, 5'-CTTGTGGATGAT-AGCGGTAA-3', 5'-AAGTGGCTACAAAGGTCCCT-3', 50.9°C. All expression ratios were normalized by the expression of GAPDH. The procedures for semiquantitative RT-PCR were as previously described,<sup>9</sup> with some modifications.

**RESULTS**

**Selection of Candidate Genes For Prediction of Lymph Node Metastasis**

SAM selected various genes showing statistically significant differences in expression level between (A) the lymph node metastasis-positive state and (B) the lymph node metastasis-negative state. Tentatively, we selected 30, 60, 90, and 120 genes by SAM, and the respective FDRs were 5.3%, 11.6%, 12.3%, and 14.2%.

### ANNs Can Predict Lymph Node Metastasis

We used four-layered, bottle-neck-shaped ANNs for prediction of lymph node metastasis. Various gene subsets selected with SAM were tested, and we found that our ANN model could predict lymph node metastasis most efficiently with 60 clones (58 genes) (Fig. 3, Table 2), although FDR was decreased (i.e., the specificity was increased) when the number of genes selected by SAM was decreased. The predictive accuracy for lymph node metastasis with 60 clones with use of ANN was 10 of 13 (77%) in newly added cases that were not used for gene selection by SAM and 24 of 28 (86%) in all cases (sensitivity: 15/17, 88%; specificity: 9/11, 82%; Az value: 0.891).

### Clustering Analysis and LMS Analysis for Prediction of Lymph Node Metastasis

Using the previously mentioned 60 clones, we performed a clustering analysis (Fig. 4) and an LMS analysis (Fig. 5). It was difficult to extract useful information for the prediction of lymph node metastasis by clustering analysis, even if the number of the clones (genes) used was changed to 30, 90, or 120 (data not shown). In contrast, predictive accuracy of LMS was 9 of 13 (69%) in newly added cases and 24 of 28 (86%) in all cases. LMS was inferior to ANN in the predictive potential for lymph node metastasis because it showed lower ability of generalization. LMS predicted lymph node-positive states accurately but could not accurately predict lymph node-negative states (sensitivity: 17/17, 100%; specificity: 7/11, 67%; Az value: 0.890) (Fig. 5). The results of LMS did not change if the number of the clones (genes) used was changed to 30, 90, or 120 (data not shown).

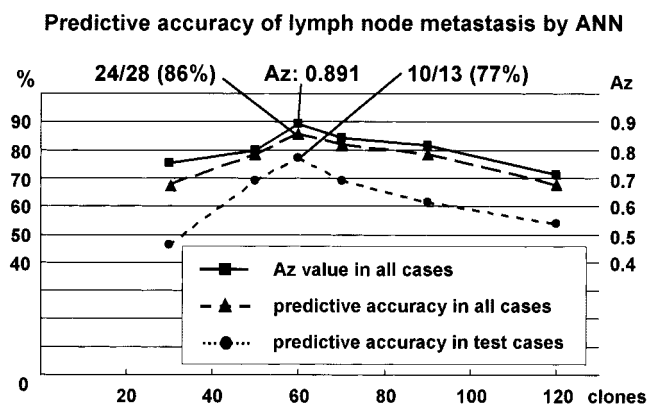


**FIG. 3.** Predictive rates in all cases, newly added test cases, and Az (area under the receiver operating characteristic curve) values show parabolic curves. The most accurate prediction was achieved at 60 clones (58 different genes), at rates of 24 of 28 (86%) in all cases and 10 of 13 (77%) in test cases. The Az value in all cases was 0.891.

### Validation of Microarray Data by Semiquantitative RT-PCR

Melting curve analysis showed a single peak, which indicated a single amplification of each target gene, and the production of single bands was also confirmed by electrophoresis (data not shown). The results of semiquantitative RT-PCR for DMN and IFNGR1 were not identical to but were correlated with the microarray data (Fig. 6).

### DISCUSSION

It has been reported that endoscopic resection, radiation therapy, and chemotherapy, alone or in combinations, are effective for the treatment of early esophageal cancers.<sup>2-4</sup> However, it is essential to recognize whether lymph node metastasis has occurred or not before the selection of these nonsurgical treatments. Lymph node metastasis in esophageal cancer rarely occurs when the primary tumor is limited within the mucosal layer; however, it occurs frequently once the tumor extends into the submucosal layer.<sup>21</sup> Therefore, surgical treatments with lymph node dissection are likely to be employed when a tumor progresses deeper than the submucosal layer. Surgery is the main therapy for esophageal cancer, and extended lymph node dissection is recommended.<sup>1</sup>

Although extensive lymph node dissection has the same level of complications as standard lymph node dissection, the procedure takes longer and results in prolonged hospital stays. On the other hand, even if the tumor invasion is beyond the submucosal layer, if there is no lymph node metastasis, it would be considered oversurgery to treat these cases with a surgical modality that involves great stresses. These dilemmas result from the lack of a diagnostic modality that can estimate lymph node metastasis accurately before any treatment. If we could predict lymph node metastasis status accurately before treatment, more precise, tailor-made therapeutic selections could be employed as treatments.

We show here that lymph node metastasis in esophageal cancers could be predicted in a high rate from microarray data with ANN analysis, although the current experimental scale was relatively small. Since Rumelhart et al.<sup>10</sup> developed Feed Forward and Error Backpropagation learning in ANN, ANN has been applied in medical research, i.e., for image processing,<sup>22</sup> diagnosis of malignancy,<sup>11</sup> and prediction of therapeutic response<sup>22</sup> and outcome.<sup>23</sup> ANN has been applied to microarray data relatively recently<sup>11</sup>; however, there has been no reported study in which ANN was applied to evaluation and prediction of lymph node metastasis on the basis of microarray data. Although ANN has disadvantages that

**TABLE 2.** Identities of 60 clones extracted with cDNA microarrays

Gene Name	Symbol	Accession Number
Relatively upregulated genes in lymph node metastasis–positive states		
Interleukin 6	IL6	NM_000600
Desmuslin	DMN	XM_031031
Jun D proto-oncogene	JUND	N66278
Serine dehydratase	SDS	XM_006645
Peroxiredoxin 2	PRDX2	NM_005809
p160	PELP1	U88153
Reproduction 8	D8S2298E	NM_005671
Purkineje cell protein 4	PCP4	NM_006198
NADH dehydrogenase (ubiquinone) 1 alpha subcomplex 7	NDUFA7	NM_005001
Amiloride-sensitive cation channel 1, neuronal (degenerin)	ACCN1	NM_001094
Glucokinase (hexokinase 4), transcript variant 1	GCK	NM_000162
Hepatocyte nuclear factor-6 alpha (HNF6)	ONCUT1	U96173
Glutathione peroxidase 4	GPX4	NM_002085
Putative sterol reductase SR-1	TM7SF2	AF096304
Homo sapiens cDNA FLJ34019 fis, clone FCBBF2002898	*	AA398289
Mitogen-activated protein kinase 8 interacting protein 1	MAPK8IP1	AI206407
Isocitrate dehydrogenase 2 (NADP+), mitochondrial	IDH2	AA679907
DKFZP434D146 protein	DKFZP434D146	NM_015595
ESTs	*	T66794
ESTs	*	H84871
Relatively upregulated genes in lymph node metastasis–negative states		
Nucleoporin 153kD	NUP153	AI568716
Dual specificity phosphatase 1	DUSP1	N62259
Peptidylprolyl isomerase C (cyclophilin C)	PPIC	AA676404
Protection of telomeres 1	POT1	NM_015450
Ligase 4, DNA, ATP-dependent	LIG4	NM_002312
KIAA1128 protein	KIAA1128	AA114107
Myogenin (myogenic factor 4)	MYOG	AI291603
CIG49 (cig49)	IFIT4	AF026939
Interleukin 1 receptor accessory protein	IL1RAP	NM_002182
Phospholipid scramblase 1	PLSCR1	AF098642
Tublin, alpha 1 (testis specific)	TUBA1	XM_050952
Cyclin A2	CCNA2	AA608568
High-mobility group protein 2	HMGB2	AA019203
Chloride channel 4	CLCN4	XM_045756
Toll-like receptor 4	TLR4	XM_057452
Transporter similar to yeast MRS2	MRS2L	AI023118
G protein beta 5 subunit	GNB5	AF017656
Interferon gamma receptor 1	IFNGR1	NM_000416
Kinesin-like 1	KNSL1	AA504625
Fas (TNFRSF6)-associated via death domain	FADD	NM_003824
Interleukin 1, beta	IL1B	NM_000576
Glucosamine (N-acetyl)-6-sulfatase	GNS	AA035347
Laminin-5, alpha3b chain	LAMA3	X84900
PTPRF, interacting protein (liprin), alpha 1	PPFIA1	N49751
Deleted in azoospermia	DAZ	AA129397
KIAA0562 gene product	KIAA0562	XM_001505
DDX17, transcript variant 2	DDX17	NM_030881
Arachidonate 5-lipoxygenase	ALOX5	NM_000698
Amyloid beta (A4) precursor protein	APP	AA128553
Nescient helix loop helix 1	NHLH1	H09936
MRS2-like, magnesium homeostasis factor ( <i>S. cerevisiae</i> )	MRS2L	AI023118
ESTs	*	H08785
ESTs, Moderately similar to T00390 KIAA0614 protein–human (fragment)	*	AA877082
DNA-binding transcriptional activator	NCYM	AA609982
Cytokine receptor-like factor 3	CRLF3	AI240562
Interferon consensus sequence binding protein 1	ICSBP1	AI391632
KIAA1128 protein	KIAA1128	AA114107
ESTs	*	H02158
Hypothetical protein DKFZp547M136 similar to widely-interspaced zinc finger motifs	LOC58525	AI360314
Homo sapiens cDNA FLJ11904 fis, clone HEMBB1000048	*	AA447098

\* Not applicable.

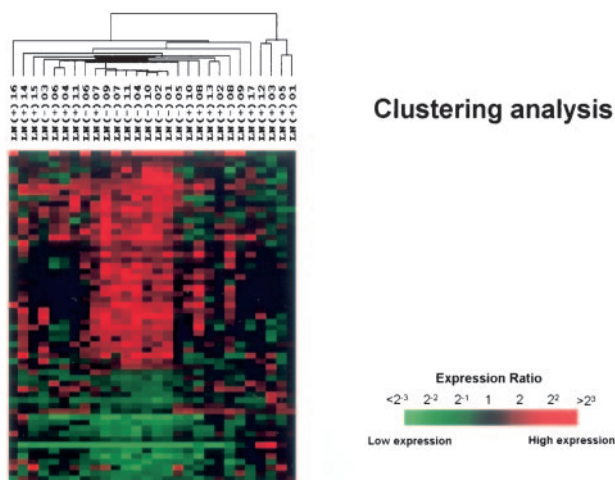


**FIG. 4.** Clustering analysis with 60 clones extracted by SAM. The color scale ranges from saturated green for  $2^{-3}$  and below to saturated red for  $2^{-3}$  and above. Each gene is represented by a single row of colored boxes; each case is represented by a single column. Branch lengths of the dendrogram show the degree of similarity between the cases. Clustering analysis does not successfully categorize the cases as lymph node metastasis-positive and -negative.

include its “black box” nature, greater computational burden, proneness to overfitting, and the empirical nature of model development,<sup>24</sup> there are many reports in which ANN still has superior potential for detecting complex nonlinear relationships between dependent and independent variables and other classic statistical techniques.<sup>22,25</sup>

### Lymph node metastasis score analysis

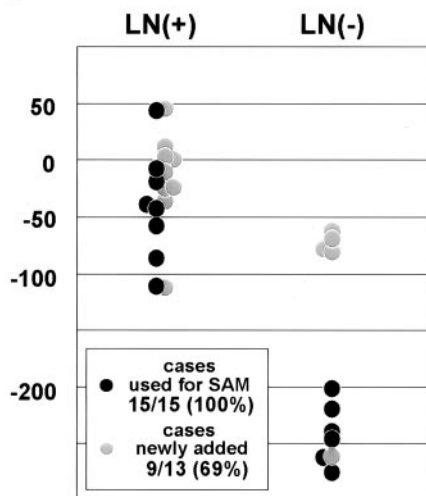


**FIG. 5.** Lymph node metastasis score (LMS) analysis with 60 clones extracted by SAM. Circles in black represent the cases used for SAM, and circles in gray represent the cases newly added. Predictive accuracy was 24 of 28 (86%) in all cases and 9 of 13 (69%) in newly added test cases. Az value in all cases was 0.890.

### Comparison with results of LightCycler

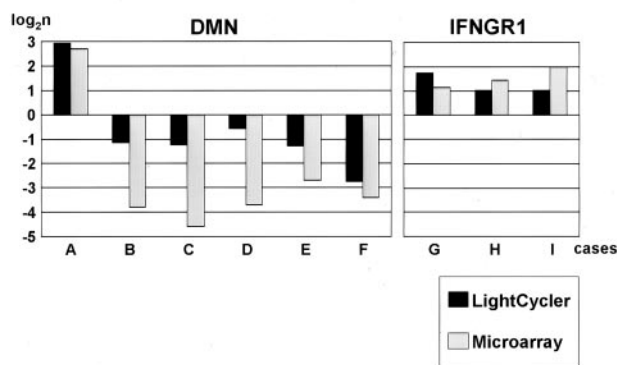


**FIG. 6.** Comparison of the results of gene expression analysis for desmuslin (DMN) and interferon gamma receptor 1 (IFNGR1) with use of microarray and LightCycler analysis. Black bars represent gene expression values from LightCycler, and gray bars represent gene expression values from microarrays. The results of semiquantitative RT-PCR for DMN and IFNGR1 were not identical to but were correlated with the microarray data.

Recently, huge amounts of data have been generated by high-throughput techniques in genomic and proteomic researches. ANN not only can implicitly reveal relationships within large sets of data but also can simultaneously deal with both variables that can be qualified (e.g., age, height, weight, length of tumor and microarray data) and those that cannot be qualified (e.g., gender, tumor type, stage of disease, family history and habit); thus, ANN is expected to lead to more useful information for clinical decision-making. With our ANN model, the 60-clone-prediction of lymph node metastasis showed the highest accuracy. As shown in Figure 3, the predictive accuracy and Az values formed approximately parabolic curves, probably because the smaller the number of genes used in ANN, the less adequate the genetic information is for predicting lymph node metastasis correctly, while with a larger number of genes, ANN likewise could not work properly, possibly because of being affected by increased biases. It seems that the accuracy of gene filtering for the phenotypes of interest is important when the number of cases analyzed by ANN is relatively small; however, in larger-scale studies, ANN could predict phenotypes more accurately because a large amount of training data lead to more correct outcomes, although a small number of irrelevant genes are inevitably included.

Hereafter, biopsy materials are to be used for prediction of lymph node metastasis, and with the enrollment of an increasing number of patients in the study, we believe that the accurate prediction of lymph node metastasis in esophageal cancer patients before any treat-

ment begins should become possible. In the near future, if we could predict lymph node metastasis accurately with use of biopsy materials, decisions about surgical treatments would be greatly influenced. For example, in a case predicted to be positive for lymph node metastasis, surgical treatment should be selected even if the patient's esophageal cancer is limited to within the mucosal layer, while in another case predicted to be negative for lymph node metastasis, nonsurgical treatment such as endoscopic resection, radiation therapy, or chemotherapy would be selected for early esophageal cancers and surgical treatments without lymph node dissection might be selected for invasive tumors. Since it would be possible to establish tailor-made therapy for such esophageal cancer patients, this predictive system would be very useful in clinical situations.

Micrometastasis<sup>26</sup> has been taken into consideration in the evaluation of lymph node metastasis in this study. We have been able to achieve highly accurate prediction of lymph node metastasis because there might exist distinctive differences in "gene signature" between primary esophageal cancers with and without lymph node metastasis, including micrometastasis. That is to say, "gene signature" that expresses certain different gene products may cause lymph node metastasis regardless of the depth of tumor invasion. Esophageal cancers with a particular gene signature may have lymph node metastasis in an early stage of tumorigenesis, whereas esophageal cancers without that gene signature may rarely have lymph node metastasis, however deep they invade into the esophageal wall. Consequently, our method may be useful in detecting lymph node metastasis, inclusive of micrometastasis.

In comparison of esophageal cancer specimens with and without lymph node metastasis, SAM did not detect genes that had been reported to be related to lymph node metastasis of esophageal cancers, such as extracellular matrix degrading enzymes (matrix metalloproteinase-2, -7, -9, and -13)<sup>27-30</sup>; cytoskeletal and adhesive molecules; E-cadherin,<sup>31</sup> alpha-catenin,<sup>31</sup> beta-catenin,<sup>32</sup> and desmoglein 1<sup>33</sup>; and growth factors (vascular endothelial growth factor<sup>34</sup> and vascular endothelial growth factor C).<sup>35</sup> However, some immunity-related genes such as cytokines and apoptosis-related molecules were detected. This implies that the key factors involved in lymph node metastasis are interactions between progressive, invasive cancer cells and their environment or host immunity that suppress tumor progression. Consequently, for the evaluation of lymph node metastasis, it is important to analyze not only cancer cells but also their environments.

Interleukin 1-beta (IL1B),<sup>36</sup> interleukin 6 (IL6),<sup>37</sup> and sterol reductase SR-1(TM7SF2)<sup>38</sup> have been reported to

be molecules positively related to lymph node metastasis. In contrast, Fas-associated death domain (FADD),<sup>39</sup> phospholipid scramblase 1 (PLSCR1),<sup>40</sup> and dual-specificity phosphatase 1 (DUSP1)<sup>41</sup> have been reported as negatively related molecules. The findings of the present study about the expression of FADD, PLSCR1, IL6, TM7SF2, and DUSP1 were consistent with those of previous reports. However, our findings about IL1B were not; indeed, there was no single gene whose expression alone could predict lymph node metastasis accurately. Therefore, the overall expression patterns and balance of expression of candidate genes for lymph node metastasis should be considered.

In this study, LMS was still inferior to ANN with respect to the ability of generalization (9 of 13, or 69%, in newly added cases). However, LMS was not at all misleading with respect to lymph node-positive states (e.g., the false-negative rate was 0%); hence, the prediction of lymph node-negative states by LMS may be more reliable than that by ANN. LMS analysis can thus be useful as a supportive method for ANN.

#### ACKNOWLEDGMENTS

The acknowledgments are available online in the full-text version at [www.annalsurgicaloncology.org](http://www.annalsurgicaloncology.org). They are not available in the PDF version.

#### REFERENCES

- Altorki N, Kent M, Ferrara C, Port J. Three-field lymph node dissection for squamous cell and adenocarcinoma of the esophagus. *Ann Surg* 2002;236(2):177-83.
- Soehendra N, Binmoeller KF, Bohnacker S, et al. Endoscopic snare mucosectomy in the esophagus without any additional equipment: a simple technique for resection of flat early cancer. *Endoscopy* 1997;29(5):380-3.
- Nemoto K, Ogawa Y, Matsushita H, et al. A pilot study of radiation therapy combined with daily low-dose cisplatin for esophageal cancer. *Oncol Rep* 2001;8(4):785-9.
- Gao XS, Qiao XY, Yang XR, et al. Late course accelerated hyperfractionation radiotherapy concomitant with cisplatin in patients with esophageal carcinoma. *Oncol Rep* 2002;9(4):767-72.
- Shimada Y, Imamura M, Watanabe G, et al. Prognostic factors of oesophageal squamous cell carcinoma from the perspective of molecular biology. *Br J Cancer* 1999;80(8):1281-8.
- Fukuda M, Hirata K, Natori H. Endoscopic ultrasonography of the esophagus. *World J Surg* 2000;24(2):216-26.
- Himeno S, Yasuda S, Shimada H, et al. Evaluation of esophageal cancer by positron emission tomography. *Jpn J Clin Oncol* 2002;32(9):340-6.
- Ross DT, Scherf U, Eisen MB, et al. Systematic variation in gene expression patterns in human cancer cell lines. *Nat Genet* 2000;24(3):227-35.
- Kan T, Shimada Y, Sato F, et al. Gene expression profiling in human esophageal cancers using cDNA microarray. *Biochem Biophys Res Commun* 2001;286(4):792-801.
- Rumelhart DE, Hinton GE, Williams RJ, et al. Learning representations by back-propagating errors. *Nature* 1986;323:533-6.

11. Xu Y, Selaru FM, Yin J, et al. Artificial neural networks and gene filtering distinguish between global gene expression profiles of Barrett's esophagus and esophageal cancer. *Cancer Res* 2002;62(12):3493-7.
12. Tusher VG, Tibshirani R, Chu G. Significance analysis of microarrays applied to the ionizing radiation response. *Proc Natl Acad Sci U S A* 2001;98(9):5116-21.
13. Eisen MB, Spellman PT, Brown PO, Botstein D. Cluster analysis and display of genome-wide expression patterns. *Proc Natl Acad Sci U S A* 1998;95(25):14863-8.
14. Kihara C, Tsunoda T, Tanaka T, et al. Prediction of sensitivity of esophageal tumors to adjuvant chemotherapy by cDNA microarray analysis of gene-expression profiles. *Cancer Res* 2001;61(17):6474-9.
15. Nagayama S, Katagiri T, Tsunoda T, et al. Genome-wide analysis of gene expression in synovial sarcomas using a cDNA microarray. *Cancer Res* 2002;62(20):5859-66.
16. Sato F, Shimada Y, Li Z, et al. Lymph node micrometastasis and prognosis in patients with oesophageal squamous cell carcinoma. *Br J Surg* 2001;88(3):426-32.
17. Selaru FM, Zou T, Xu Y, et al. Global gene expression profiling in Barrett's esophagus and esophageal cancer: a comparative analysis using cDNA microarrays. *Oncogene* 2002;21(3):475-8.
18. Yang YH, Dudoit S, Luu P, et al. Normalization for cDNA microarray data: a robust composite method addressing single and multiple slide systematic variation. *Nucleic Acids Res* 2002;30(4):e15.
19. Wittwer CT, Ririe KM, Andrew RV, et al. The LightCycler: a microvolume multisample fluorimeter with rapid temperature control. *Biotechniques* 1997;22(1):176-81.
20. Rychlik W, Rhoads RE. A computer program for choosing optimal oligonucleotides for filter hybridization, sequencing and in vitro amplification of DNA. *Nucleic Acids Res* 1989;17(21):8543-51.
21. Nishimaki T, Tanaka O, Suzuki T, et al. Tumor spread in superficial esophageal cancer: histopathologic basis for rational surgical treatment. *World J Surg* 1993;17(6):766-71; discussion, 771-2.
22. Biagiotti R, Desii C, Vanzi E, Gacci G. Predicting ovarian malignancy: application of artificial neural networks to transvaginal and color Doppler flow US. *Radiology* 1999;210(2):399-403.
23. Marchevsky AM, Patel S, Wiley KJ, et al. Artificial neural networks and logistic regression as tools for prediction of survival in patients with Stages I and II non-small cell lung cancer. *Mod Pathol* 1998;11(7):618-25.
24. Tu JV. Advantages and disadvantages of using artificial neural networks versus logistic regression for predicting medical outcomes. *J Clin Epidemiol* 1996;49(11):1225-31.
25. Bottaci L, Drew PJ, Hartley JE, et al. Artificial neural networks applied to outcome prediction for colorectal cancer patients in separate institutions. *Lancet* 1997;350(9076):469-72.
26. Hosch S, Kraus J, Scheunemann P, et al. Malignant potential and cytogenetic characteristics of occult disseminated tumor cells in esophageal cancer. *Cancer Res* 2000;60(24):6836-40.
27. Koyama H, Iwata H, Kuwabara Y, et al. Gelatinolytic activity of matrix metalloproteinase-2 and -9 in oesophageal carcinoma; a study using in situ zymography. *Eur J Cancer* 2000;36(16):2164-70.
28. Yamashita K, Mori M, Shiraishi T, et al. Clinical significance of matrix metalloproteinase-7 expression in esophageal carcinoma. *Clin Cancer Res* 2000;6(3):1169-74.
29. Sato F, Shimada Y, Watanabe G, et al. Expression of vascular endothelial growth factor, matrix metalloproteinase-9 and E-cadherin in the process of lymph node metastasis in oesophageal cancer. *Br J Cancer* 1999;80(9):1366-72.
30. Etoh T, Inoue H, Yoshikawa Y, et al. Increased expression of collagenase-3 (MMP-13) and MT1-MMP in oesophageal cancer is related to cancer aggressiveness. *Gut* 2000;47(1):50-6.
31. Kadowaki T, Shiozaki H, Inoue M, et al. E-cadherin and alpha-catenin expression in human esophageal cancer. *Cancer Res* 1994;54(1):291-6.
32. Zhou XB, Lu N, Zhang W, et al. [Expression and significance of beta-catenin in esophageal carcinoma]. *Ai Zheng* 2002;21(8):877-80.
33. Nakano S, Baba M, Natsugoe S, et al. Detection of lymph node metastasis using desmoglein 1 expression in superficial esophageal cancer in relation to the endoscopic mucosal resection. *Dis Esophagus* 1998;11(3):157-61.
34. Uchida S, Shimada Y, Watanabe G, et al. In oesophageal squamous cell carcinoma vascular endothelial growth factor is associated with p53 mutation, advanced stage and poor prognosis. *Br J Cancer* 1998;77(10):1704-9.
35. Noguchi T, Takeno S, Shibata T, et al. VEGF-C expression correlates with histological differentiation and metastasis in squamous cell carcinoma of the esophagus. *Oncol Rep* 2002;9(5):995-9.
36. von Biberstein SE, Spiro JD, Lindquist R, Kreutzer DL. Interleukin-1 receptor antagonist in head and neck squamous cell carcinoma. *Arch Otolaryngol Head Neck Surg* 1996;122(7):751-9.
37. Dong G, Chen Z, Kato T, Van Waes C. The host environment promotes the constitutive activation of nuclear factor-kappaB and proinflammatory cytokine expression during metastatic tumor progression of murine squamous cell carcinoma. *Cancer Res* 1999;59(14):3495-504.
38. Matar P, Rozados VR, Roggero EA, Scharovsky OG. Lovastatin inhibits tumor growth and metastasis development of a rat fibrosarcoma. *Cancer Biother Radiopharm* 1998;13(5):387-93.
39. Shin MS, Kim HS, Lee SH, et al. Alterations of Fas-pathway genes associated with nodal metastasis in non-small cell lung cancer. *Oncogene* 2002;21(26):4129-36.
40. Silverman RH, Halloum A, Zhou A, et al. Suppression of ovarian carcinoma cell growth in vivo by the interferon-inducible plasma membrane protein, phospholipid scramblase 1. *Cancer Res* 2002;62(2):397-402.
41. Fernandez M, Eng C. The expanding role of PTEN in neoplasia: a molecule for all seasons? [Commentary re: M. A. Davies, et al. Adenoviral-mediated expression of MMAC/PTEN inhibits proliferation and metastasis of human prostate cancer cells. *Clin Cancer Res* 2002;8(6):1695-8.] *Clin Cancer Res* 2002;8:1904-14.